Density Fluctuations in a Flame in a Kármán Vortex Sheet

Izak Namer*
Drexel University, Philadelphia, Pennsylvania
Robert G. Bill Jr.†
Columbia University, New York, New York
Lawrence Talbot‡
University of California, Berkeley, California
and
Frank Robben§
Lawrence Berkeley Laboratory, Berkeley, California

The interaction of a premixed C_2H_4-air flame with a Kármán vortex street was studied. Rayleigh scattering was used to measure total gas density. Density statistics obtained from Rayleigh scattering measurements were compared with predictions by the Bray-Moss-Libby (B-M-L) model which neglects intermediate states. Density fluctuations were overpredicted by the B-M-L model by a small amount for Reynolds numbers 73 and 110. The flame was essentially a wrinkled-laminar flame for these conditions. However, for Reynolds number 500 the flame consisted of a distributed reaction zone and intermediate states accounted for as much as 80% of all states encountered in positions of the flame. The B-M-L model significantly overpredicted density fluctuation intensities for this condition.

Introduction

THE effects of fluid mechanical turbulence on premixed combustion, most apparent of which are the large increases in effective flame speeds and volumetric burning rates, have been studied both theoretically and experimentally for many years. these studies are extensively reviewed by Karlovitz,[1] Scurlock and Grover,[2] Williams,[3] and Andrews et al.[4] However, progress has been impeded by a limited understanding of turbulence, even in isothermal flows, as well as by the lack of diagnostic probes capable of providing accurate time-resolved velocity, density, temperature, and concentration fields in a combustion environment. Recently, Rayleigh scattering has been developed as a nonintrusive diagnostic technique to measure space- and time-resolved density.[5-7] This technique was applied in the present study to investigate the interaction of a premixed flame with a Kármán vortex sheet. The motivation for this study was that the vortex street represents an unsteady flow consisting of large eddies. If the eddies which form the vortex street are very large compared to the laminar flame thickness δ, an unsteady wrinkled flame can be produced. Such flames could be analyzed with models designed for turbulent wrinkled-laminar flames.[8,9] This is because, as first described by Damkohler,[10] to such turbulent flames the approach flow would appear as simply an unsteady but laminar flow. By studying the flame in a vortex street, rather than in a fully turbulent flow, the observations are not encumbered by strong three-dimensional effects such as streamwise vortices (the vortex street is largely two dimensional) nor by the effects of spectrum of length scales which exist in a truly turbulent flow. It should be remembered, however, that the features which make this experiment attractive result in simplified circumstances which are not directly comparable to any turbulent flow. In this respect the experiment is limited, but not any more so than other experiments might be. Nevertheless, this study represents an important contribution to the understanding of unsteady flame propagation and wrinkled-laminar flames.

Damkohler[10] was the first to study the effect of turbulence on flame propagation. He defined two limiting conditions. The first occurs at relatively low Reynolds numbers[4,11] where the length scales of the turbulence are much larger than the laminar flame thickness. The effect of turbulence in this case is simply to wrinkle an otherwise laminar flame (hence, the name "wrinkled-laminar flame model") and increase the effective flame speed by increasing the flame's surface area. The second regime occurs at Reynolds numbers for which the length scales are smaller than the flame thickness. In this case, the turbulence serves to increase heat and mass transport within the reaction zone. It has been suggested[12] that for this regime the effect of turbulence may be modeled by replacing molecular diffusivities by turbulent eddy diffusivities. These and other models based on the original ideas of Damkohler have had limited success in correlating experimental data. Karlovitz et al.,[13] for example, obtained results which indicate increased burning rates not accountable by these theories and suggested that the flame was itself a source of turbulence. The concept of flame-generated turbulence has been subscribed to by various researchers.[14-16] Others,[17-20] however, suggest that discrepancies in the predictions of the wrinkled flame model are due to large errors in most measurements of turbulent flame speed. Since the concept of flame-generated turbulence was invoked to explain the available data, it may be that the data were interpreted incorrectly and the concept of flame-generated turbulence may be inappropriate. Therefore, the wrinkled-laminar flame model may yet be a reasonable first approximation of some turbulence-combustion interactions. It appears possible that models, with suitable modifications of the wrinkled-laminar flame concept of turbulent flame propagation which do not

Received March 2, 1982; revision submitted April 19, 1983.

*Assistant Professor, Department of Mechanical Engineering and Mechanics. Member AIAA.
†Assistant Professor, Department of Mechanical Engineering. Member AIAA.
‡Professor, Department of Mechanical Engineering. Member AIAA.
§Senior Scientist. Member AIAA.

invoke flame-generated turbulence, may give a more detailed understanding of the wrinkling process. One promising model is the so called Bray-Moss-Libby probability density model, discussed subsequently. This model can be applied to unsteady as well as turbulent flame propagation and is a good candidate for qualitative and quantitative comparison with these experiments.

The wake behind a cylinder of diameter D in a stream of velocity U for Reynolds numbers ($Re_D = UD/\nu$) between 40 and 5000 exhibits a fairly regular pattern of alternately rotating vortices known as a Kármán vortex street. This phenomena has been studied extensively by many investigators (see the review by Marris[21] and Lamb[22]). Friehe,[23] Nishioka and Sato,[24] Kovasznay,[25] Tritton,[28] and Roshko,[26,27] among others, have measured the variation of the vortex shedding frequency f with Reynolds number and provided considerable data on the dependence of the Strouhal number ($St = fD/U$) on the Reynolds number. Kovasznay[25] and Roshko[26] found that a stable, regular vortex street is obtained only for Reynolds numbers between 40 and 150. Various authors quote different values of the upper limit. This may be due to the fact, not generally realized, that for Reynolds numbers below a critical value the vortex street is not shed from the cylinder but develops from a laminar wake instability.[21,25,28] When the Reynolds number increases to some critical value, there is a transition and the vortices begin to be shed directly from the cylinder. In this transition regime vortex shedding becomes irregular but becomes regular again once beyond it until the wake becomes turbulent. Tritton[28] and Marris[21] suggest that the critical value of Reynolds number for this transition is about 90. During this study this transition was observed over a range of Reynolds numbers as low as 75. The data of Roshko[26] suggest that he may have observed this phenomenon at a Reynolds number of 150, although he attributed his observations to scatter in the data and not to a fundamental change in the fluid dynamics. In any case, above $Re_D = 150$ the wake starts to become irregular as turbulence appears. By $Re_D = 300$ the wake is reasonably turbulent while the dominant velocity fluctuations remain around the vortex shedding frequency.

A schematic of the problem studied is shown in Fig. 1. The fuel used was ethylene, C_2H_4, for all the cases studied. The three conditions at which measurements were made are summarized in Table 1. Table 1 shows that two cases studied correspond to Re_D below which turbulence first appears, whereas the third case ($Re_D = 500$) corresponds to a wake with substantial turbulent motion. One might expect the flame in this latter wake to be different from a wrinkled flame. In contrast, the two former cases should lead to a wrinkled-laminar flames. These expectations are, in fact, confirmed by the results presented in this paper. Rayleigh scattering was used to measure the instantaneous gas density. From these measurements statistical moments of density, such as the mean and the root-mean-square (rms), as well as spectra and pdf's were calculated and analyzed.

In addition to the measurements and calculations mentioned, a comparison was made with the predictions of the Bray-Moss-Libby model[15,29,30] for density statistics. Implications of the formulation used in the B-M-L model are discussed by Pope.[31] Some of the pertinent aspects of the B-M-L model are summarized next.

B-M-L Model

Bray, Moss, and Libby introduce a probability function P for the product concentration at a location r such that

$$P(r,c) = \alpha(r)\delta(c) + \beta(r)\delta(c-1) + [\eta(c) - \eta(c-1)]\gamma(r)f(c) \quad (1)$$

Here c is the reaction progress parameter and is defined by

$$\rho/\rho_u = (1+\tau c)^{-1} \quad (2)$$

$$\tau = (\rho_u/\rho_b) - 1 \quad (3)$$

ρ_u and ρ_b are the densities of the unburned and burned gases, respectively. The functions $\delta(c)$ and $\eta(c)$ are the Dirac delta and Heaviside functions, respectively. The coefficients $\alpha(r)$, $\beta(r)$, and $\gamma(r)$ represent the reactant, product, and intermediate state probabilities, respectively, and $f(c)$ is a continuous function of product mass fraction through the

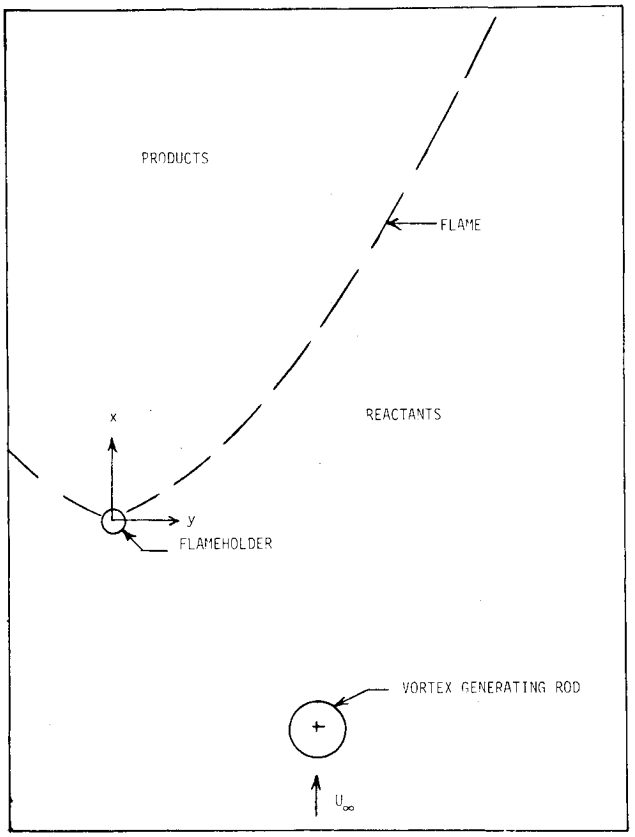

Fig. 1 Schematic of flame interaction with a Kármán vortex street.

Table 1 Experimental conditions

U, cm/s	D, mm	Re_D	ϕ	y_c, mm	Data rate, samples/s	f_s, Hz
55.0	2.0	73	0.52	12.5	1.0	23±4
55.0	3.0	110	0.52	12.5	1.0	23±4
250.0	3.0	500	0.5	10.0	2.0	171±8

N.B.: U = flow velocity, D = diameter of vortex generating cylinder, $Re_D = UD/\nu$ = Reynolds number of vortex generating cylinder based on the viscosity of the reactants at room temperature, ϕ = equivalence ratio, y_c = lateral distance between the flameholder and the vortex generating cylinder, f_s = dominant frequency in spectrum of Rayleigh scattering in flame.

flame. It follows that if

$$\int_0^1 f(c)\,dc = 1 \tag{4}$$

then,

$$\alpha(r) + \beta(r) + \gamma(r) = 1 \tag{5}$$

The term "intermediate states" refers to conditions where the density is different than either the unburned or fully burned gas densities and not just to intermediate chemical states. In applying the model infinitely fast chemistry is assumed ($\gamma \ll 1$) and, hence, $\alpha + \beta \approx 1$. Bray and Moss[30] comment that the approximation of negligible intermediate states "should be applicable to situations where wrinkled-laminar flame and related physical models are valid. On the other hand, if combustion corresponds more closely to a distributed reaction model, (intermediates) will tend to be large, and the ...approximation will not be valid...." Nevertheless, analysis usually continues with a small γ approximation because it is then not necessary to say anything about $f(c)$. This is a significant simplification since it then follows that

$$\alpha = 1 - \beta = \frac{1 - \tilde{c}}{1 + \tau\tilde{c}} \tag{6}$$

and

$$\beta = \left(\frac{1+\tau}{1+\tau\tilde{c}}\right)\tilde{c} \tag{7}$$

where $\tilde{c}$, the Favre-averaged reaction progress parameter, is obtained from

$$\tilde{c} = \frac{1}{\bar{\rho}}\int_0^1 P\rho\,dc = \frac{1}{\tau}\left(\frac{\rho_u}{\bar{\rho}} - 1\right) \tag{8}$$

Then, the intensity of density fluctuations is no longer a function of r but is given by

$$\frac{(\overline{\rho'^2})^{1/2}}{\rho_u} = \frac{\bar{\rho}}{\rho_u}\tau\left[\frac{\tilde{c}(1-\tilde{c})}{1+\tau}\right]^{1/2} \tag{9}$$

The B-M-L model continues by predicting further density statistics and other important results. However, we are interested here in the ability of Eq. (9) to predict the density fluctuation intensity in a flame in a Kármán vortex street and the validity of the small γ approximation for this flow. In the present experiment the quantities $\tilde{c}$, $\bar{\rho}$, $(\overline{\rho'^2})^{1/2}$, and τ were measured and compared with Eq. (9).

It should be noted that Eqs. (6-9) impose no restriction on the turbulence or the character of the flow. The only assumption involved is that the flame be treated as a flame sheet and intermediate states neglected. This assumption is more valid for wrinkled-laminar flames than for highly turbulent flames where there will be a thicker, more diffuse reaction zone. Since Libby and Bray[29] apply this model to highly turbulent flames, their predictions may be somewhat less accurate. However, since some of the flames considered here should be in the wrinkled-laminar flame regime, the flame sheet approximation seems appropriate and Eqs. (6) and (9) may be valid.

Experimental Method

The experimental apparatus has been described in detail in Refs. 20 and 32-35. A coaxial jet was used as an open jet wind tunnel. Premixed ethylene-air was supplied from a 200-mm-diam × 400-mm-long stagnation chamber to the inner jet through a 51-mm-diam nozzle. An outer coaxial annular jet, of outside diameter of 102 mm, was used to shield the inner flow from the surrounding room air. The flow velocities of the two jets were matched. The vortex generating rod was placed just beyond the nozzle exits. The flame was stabilized on a 1-mm-diam rod whose axis was parallel to that of the vortex generating rod. The relative locations of the two rods are indicated in Fig. 1 and Table 1 which summarizes the experimental conditions.

The Rayleigh scattering system used has been described in Refs. 20, 33, and 35. A Spectra Physics argon ion laser operating at the 488-nm line was used as the light source. The output power was 0.8 W. The laser beam was focused to a 40-μm waist by two lenses. The probe volume was about 1 mm long and 40 μm in diameter with its axis parallel to the flame holder and the vortex generating rod. The 40-μm diameter represents less than about 1/20th the thickness of the laminar flame. Therefore, these probe volume dimensions are sufficient to resolve the thin reaction zones so long as there are no significant spatial variations along the axis of the probe volume. Roshko[26,27] found that the length scale of axial variations of a vortex street about 18 diameters. Since the vortex generating rod diameters were 2 and 3 mm, the wavelength of axial variations along the vortex street would be about 40 or 50 mm and 1 mm long probe volume was considered to be adequate. Rayleigh scattering was collected at 90 deg from the beam direction by an f/1.2, 55-mm Olympus camera lens. The effective f number was 2.7. The collected light was spatially filtered by a 50 μm × 1 mm slit and optically filtered by a 1-nm bandpass filter centered at 488 nm. The light was focused on a RCA 931A photomultiplier whose output was amplified by an electrometer with a bandpass from dc to 1.9 KHz (−3 db corner). The Rayleigh scattering intensity was normalized by the Rayleigh scattering from the cold reactants whose density was known. This procedure simplified the calibration of the system. Namer et al.[36] have shown that for the conditions of these experiments, the Rayleigh scattering is proportional to density to an accuracy of better than 5%. Therefore, if I_R is the Rayleigh scattering intensity

$$I_R / I_{Ru} \approx \rho/\rho_u \tag{10}$$

Considerations of the properties of a Kármán vortex street, the laminar flame propagation speed, flame stability, and the physical dimensions of the experimental apparatus established constraints on the range of operating conditions. For instance, two flow velocities and two cylinders were required to generate the vortex street at different frequencies. The cylinder diameters were necessarily small (2.0 and 3.0 mm) to maintain the large length-diameter ratios (45 and 30, respectively) needed to obtain, essentially, a two-dimensional flowfield. The flow velocities used were 55 and 250 cm/s. Thus, for $U = 55$ cm/s, the Reynolds numbers were 73 and 110 for the 2- and 3-mm rods, respectively. For the flow velocity $U = 250$ cm/s the 3-mm rod was used to generate the vortex street. The Reynolds number for this condition was 500. In order to get stable flame propagation and avoid flashback or blowoff an equivalence ratio of 0.52 was chosen when $U = 55$ cm/s ($Re_D = 73$ and 110). The equivalence ratio was 0.5 when $U = 250$ cm/s ($Re_D = 500$). Furthermore, as illustrated in Fig. 1, the cylinder had to be placed upstream of the flameholder in order to prevent the flame from attaching itself to the vortex generating cylinder. The flameholder was located at the origin of the coordinate system used. Denoting the coordinates of the vortex generating cylinder location as (x_c, y_c), x_c was −25.0 mm and y_c is tabulated in Table 1 for each case studied. The compromises required for the stable operation of the experiment limited the range over which parameters could be varied. Nevertheless, the data presented are important in judging models and suggesting directions for further experiments.

As described in the literature, it was found that the regularity of the vortex street was enhanced by reducing three-

dimensional end effects. This was achieved by putting 2 cm square end plates, made of cardboard, on the cylinders to isolate the interaction betwen the cylinder and the edge of the jet.

The experimental apparatus was mounted on a three-axis traverse operated by separate stepping motors which were computer controlled. Thus, the flowfield positions could be scanned automatically for the Rayleigh scattering. Profiles of density were obtained by scanning in the y direction for a particular x location. When the profile was completed the test section was moved to a new x location for the next profile. The distance, in x, between profiles was 5 mm. Data acquisition was begun in the region of cold reactants. An adjusting grid was used so that 1.5-mm steps were taken in the y direction outside the flame and 0.5-mm steps inside the flame. To accomplish this the mean signal level from 100 samples was calculated and compared with the mean at the previous location. If the mean was less than 80% of the previous mean, the test section was backed up 1 mm and the spacing was set to 0.5 mm.

Measurements were obtained using 12 bit A/D converter. Samples were acquired at a constant sampling rate through clock control. Raw data could be stored in disk memory files or on a 7-track magnetic tape for postprocessing with either a PDP 11/10 or the Lawrence Berkeley Laboratory CDC 7600. The data rate was 1.0 or 2.0 kHz (see Table 1) as required for each particular case. There were 5030 samples per location taken.

Results of Density Measurements

The typical density profile through a flame, obtained from Rayleigh scattering measurements is shown in Fig. 2. All densities were normalized by the density of the cold reactants which were at room temperature. Recall that the flameholder was located at $y=0$. The flame is identified by the gradient in mean density seen here in the region $20 \lesssim y \lesssim 30$ mm. This is also the region where large density fluctuations were found as a consequence of the flame fluctuations. The peak in density fluctuations occurs at approximately the location where the mean density is one half the unburned gas density. The ratio of the burned gas density to the unburned gas density is 0.2 and, therefore, from Eq. (2) $\tau=4$. Figures 3 and 4 illustrate the evolution of the mean and rms density profiles, for the various conditions studied, as a function of streamwise location x. An increase in flame thickness with x is evident in both the mean and rms profiles. The flame thermal thickness for the undisturbed flames (no vortex street) was <1.0 mm as determined from Rayleigh scattering profiles. The formation

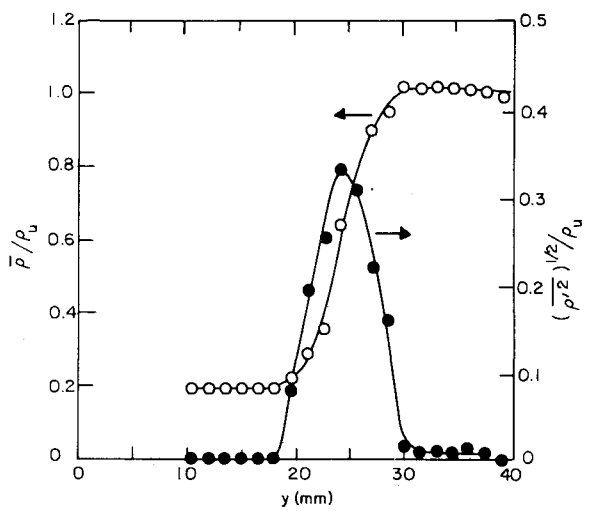

Fig. 2 Normalized mean and rms density profile through a flame.

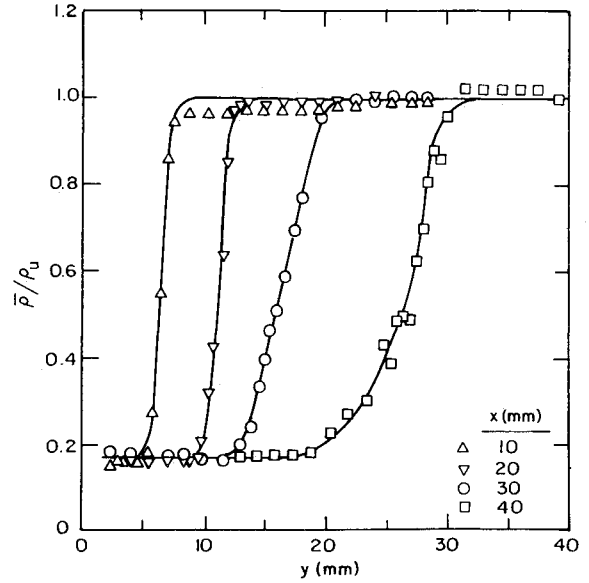

a) $U=55$ cm/s, $\phi=0.52$, $D=2.0$ mm.

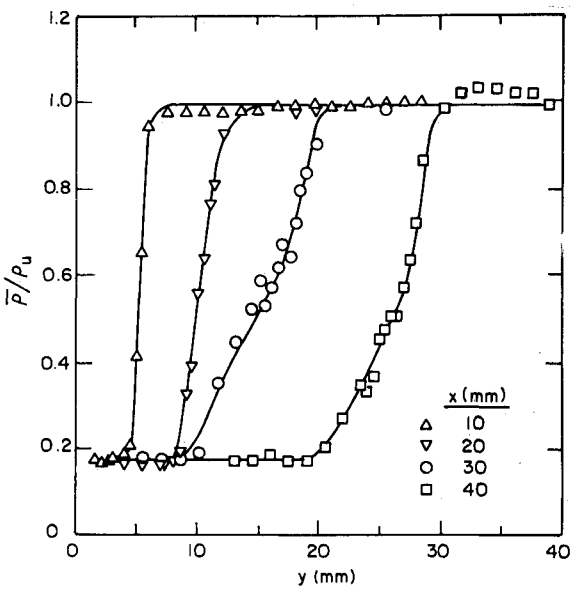

b) $U=55$ cm/s, $\phi=0.52$, $D=3.0$ mm.

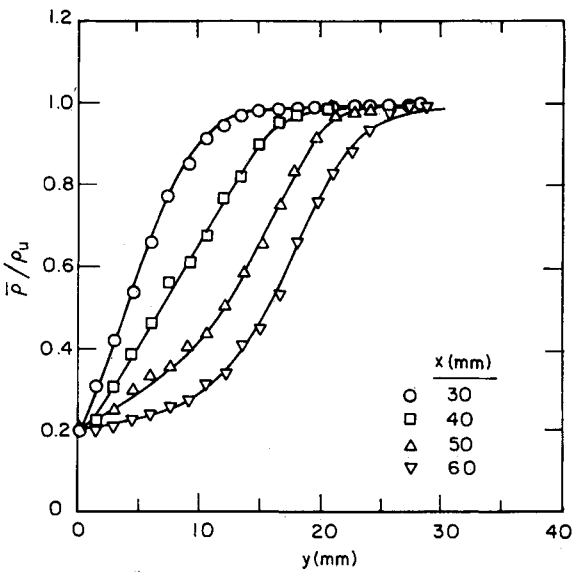

c) $U=250$ cm/s, $\phi=0.50$, $D=3.0$ mm.

Fig. 3 Mean density profiles through a flame.

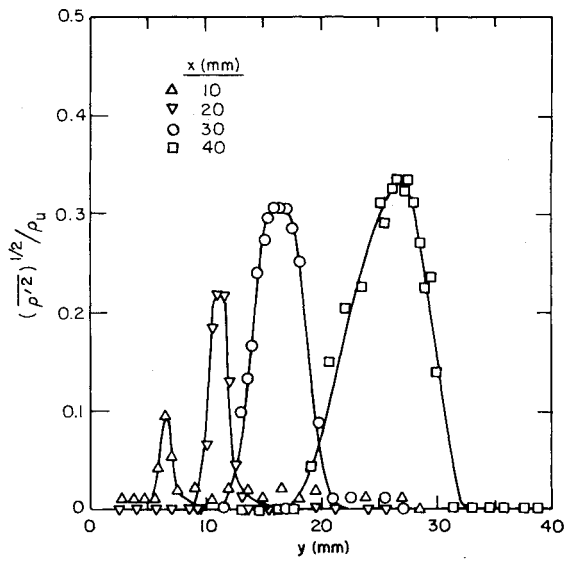

a) $U = 55$ cm/s, $\phi = 0.52$, $D = 2.0$ mm.

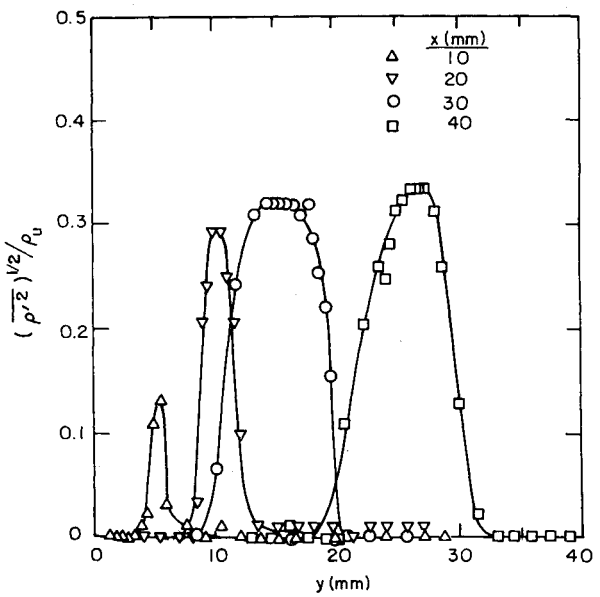

b) $U = 55$ cm/s, $\phi = 0.52$, $D = 3.0$ mm.

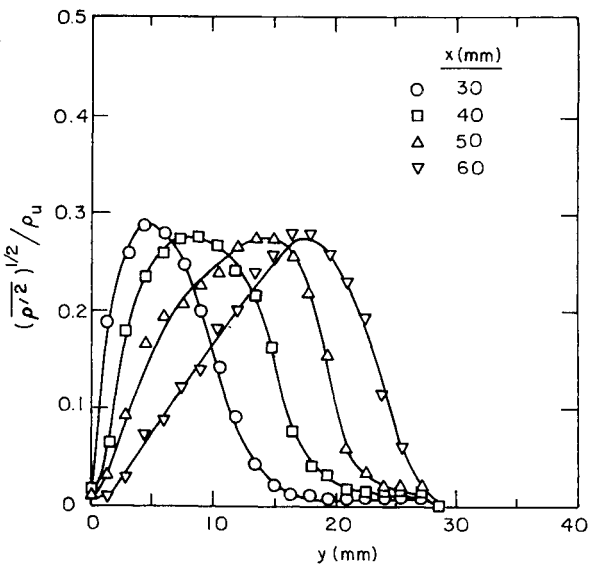

c) $U = 250$ cm/s, $\phi = 0.50$, $D = 3.0$ mm.

Fig. 4 rms density profiles through flame.

of what could be termed the flame brush is apparant from these profiles. Furthermore, the mean position of the flame was altered when the vortex street was introduced. This may be seen in Figs 5a and b. For the two cases of lower vortex shedding cylinder Reynolds number ($Re_D = 73$ and 110) shown in Fig. 5a the mean flame position moved upstream from its undisturbed location ($D = 0$) when the vortex generating rod was absent. For $Re_D = 500$, shown in Fig. 5b, the effect of the vortex street on the flame was much more pronounced. The flame brush became much thicker, approximately 20 mm thick. Surprisingly, the mean flame position was downstream of the undisturbed flame. This shift may have been due to a change in the nature and character of the flow in the vicinity of the flameholder caused by the introduction of the vortex street. However, this could not be determined from the available data. It was observed that the flame formed a cusp at the flameholder of this case and appeared concave whereas a cusp was not observed for the other cases. Power spectra of density fluctuations were calculated and showed that for all three cases the peak in the spectrum of density fluctuations correlated well with the vortex shedding frequency. The dominant frequencies of density fluctuations for the conditions investigated are given in Table 1.

As discussed, the Favre-averaged reaction progress parameter $\tilde{c}$ may be determined at each location from the mean density $\bar{\rho}$. The theoretical evolution of the density fluctuation, $(\overline{\rho'^2})^{1/2}/\rho_u$ with $\tilde{c}$ was computed from Eq. (9) for $\tau = 4.0$ and compared with the experimental results in Figs. 6a and b. It was found that the density fluctuations correlated very well with $\tilde{c}$ in all cases. However, for all conditions studied the theory overpredicts the fluctuations in density. The maximum fluctuation intensity is overestimated by about 10% for the lower Reynolds number cases shown in Fig. 6a. The discrepancy is not too severe and indicates that the fluctuations in these flames can be modeled with reasonable accuracy by the B-M-L model and by neglecting intermediate states. However, for the $Re_D = 500$ case shown in Fig. 6b, when the flame brush was 20 mm thick and appeared to consist of a distributed reaction zone, intermediate states cannot be neglected. If they are neglected, the maximum density fluctuation intensities are overpredicted by about 30%. One might hope that an effective heat release parameter τ could be found to correlate the data in Figs. 6a and b. However, this was not possible and an analysis based on more accurate pdf's is evidently required.

To aid in the search for more accurate distribution functions, pdf's of density were measured to determine their evolution through the flame and the implication of their behavior in regards the B-M-L model. The evolution of the pdf's with $\tilde{c}$ for $Re_D = 73$ can be seen in Fig. 7. Pdf's obtained for the other cases looked very similar. Note that at $\tilde{c} = 0$ only cold reactants are present. The pdf at this location is slightly broadened by photomultiplier noise. Although the density statistics were corrected for this and other sources of errors according to Refs. 33-35, the photomultiplier noise was not removed from the pdf's. If the noise was removed, one would find a Dirac delta function at $\rho/\rho_u = 1.0$ ($\tilde{c} = 0$). Nevertheless, the essential features of the pdf's are illustrated. As $\tilde{c}$ increases, the probability of encountering intermediate states and hot products first increases until the rear of the flame is approached where one expects to find 100% hot products, although the curves in Fig. 7 were not extended far enough to show this. The biomodal nature of the distribution inside the flame can also be observed.

Analysis of the pdf's indicated that there are values of $\tilde{c}$ for which the probability of intermediate states is significant. The values of α, β, γ were estimated from the measured pdf's. The value of γ was estimated by assuming that intermediate states correspond to values of density (ρ/ρ_u) such that

$$(\rho/\rho_u)_M > (\rho/\rho_u) > (\rho/\rho_u)_m \qquad (11)$$

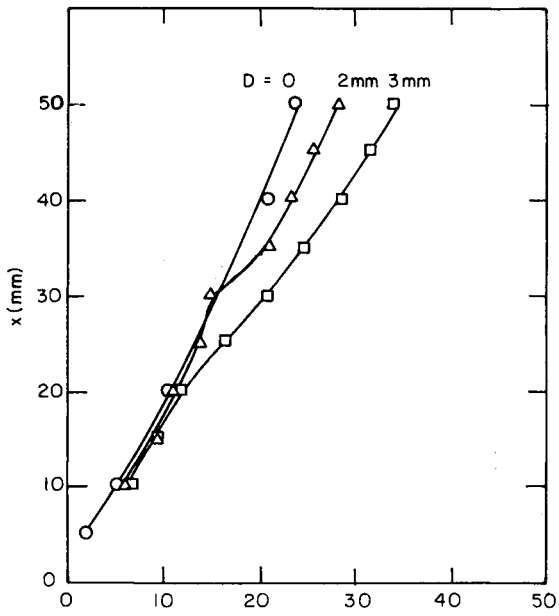

a) $U = 55$ cm/s, $\phi = 0.52$, $D = 0.0$, 2.0, and 3.0 mm.

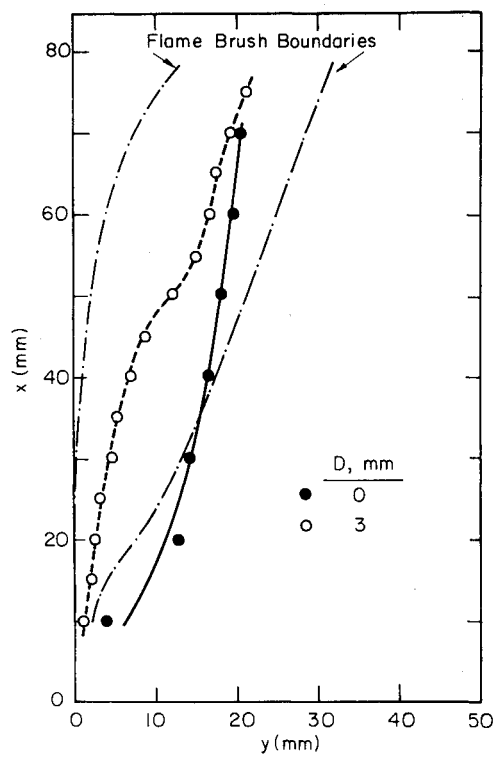

b) $U = 250$ cm/s, $\phi = 0.50$, $D = 0.0$ and 3.0 mm and flame brush thickness for $D = 3.0$ mm.

Fig. 5 Mean flame location.

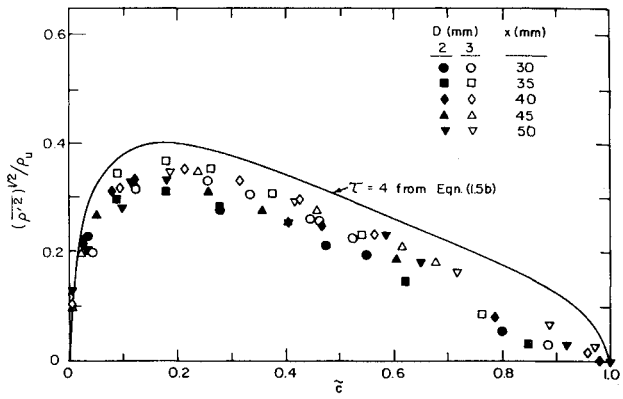

Fig. 6a $(\overline{\rho'^2})^{1/2}/\rho_u$ vs $\tilde{c}$: $U = 55$ cm/s, $\phi = 0.52$, $\tau = 4$.

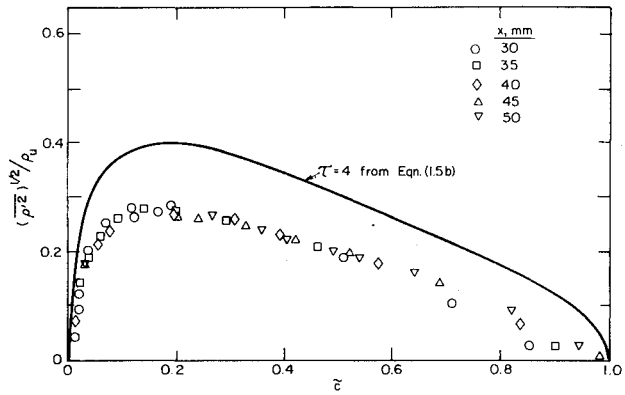

Fig. 6b $(\overline{\rho'^2})^{1/2}/\rho_u$ vs $\tilde{c}$: $U = 250$ cm/s, $D = 3.0$, $\tau = 4$.

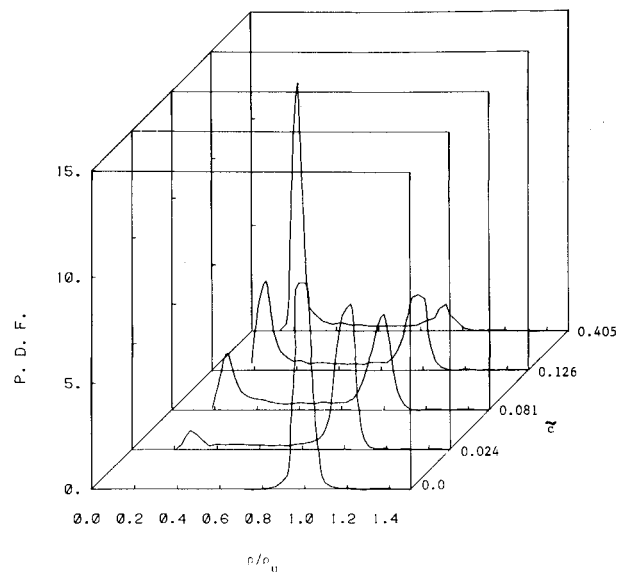

Fig. 7 Evolution of pdf of density with $\tilde{c}$: $U = 55$ cm/s, $D = 2.0$ mm, $Re_D = 73$.

where $(\rho/\rho_u)_M$ is the minimum value of the signal from cold reactants broadened by photomultiplier noise and $(\rho/\rho_u)_m$ is the maximum value of the signal from hot products broadened by photomultiplier noise. The values used were $(\rho/\rho_u)_M = 0.9$ and $(\rho/\rho_u)_m = 0.27$. Therefore, PMT shot noise made no contribution to the measured values of γ, but could have possibly led to interpreting an intermediate state as either cold reactants or hot products. In this sense the evaluation of γ might have been greater but not smaller. The values of α, β, and γ are plotted in Figs. 8a, b, and c as a function of $\tilde{c}$ for $Re_D = 73$, 110, and 500, respectively. As can be seen from these figures, the value of γ became as large as 0.4 and 0.5 in the $Re_D = 73$ and 110 flames; which means that at some locations in the flame the probability of encountering intermediate states can be 40 or 50%. Recall that these are the flames most likely to correspond to wrinkled-laminar flames and, hence, the flame sheet approximation should be most applicable. The data shown in Fig. 6a for these cases indicated that the flame sheet approximation is a fairly good assumption to make for the purpose of predicting density fluctuation intensities, and an upper bound on expected levels which was

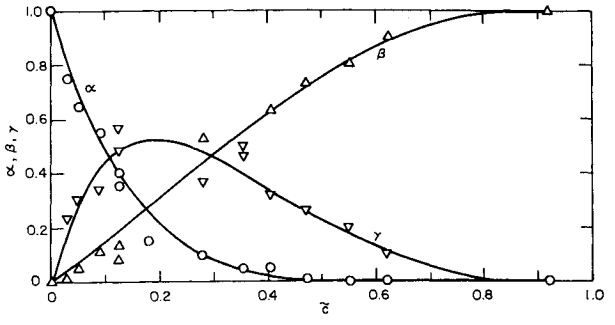

a) $U = 55$ cm/s, $D = 2$ mm.

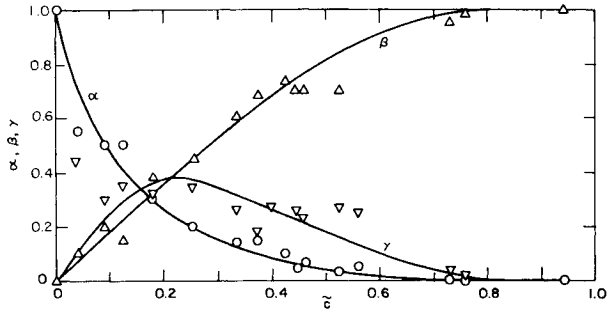

b) $U = 55$ cm/s, $D = 3$ mm.

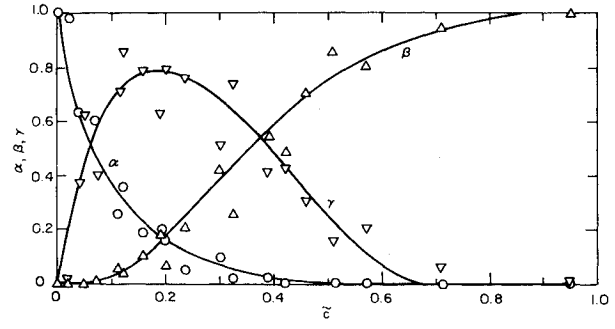

c) $U = 250$ cm/s, $D = 3$ mm.

Fig. 8 Evolution of α, β, and γ with $\tilde{c}$.

not too far from the actual fluctuation level was obtained. However, for the case of $Re_D = 500$, γ can reach 0.8 and the probability of encountering intermediates was as high as 80%, more than for products and reactants combined. The flame sheet model here is evidently a poor predictor of statistical properties in the flame.

A question which may be raised is whether the frequency response of the electrometer is responsible for the apparent large values of γ. To resolve this question power spectra of the Rayleigh scattering signal were computed. The power spectrum of the electrometer output for $Re_D = 500$ and at a location for which $\tilde{c} = 0.19$ is shown in Fig. 9. This figure shows a peak at about 171 Hz which corresponds to the vortex shedding frequency for $Re_D = 500$. The power spectrum falls off rapidly beyond 350 Hz and is down by about two orders of magnitude from the peak by 500 Hz. This indicates that the electrometer frequency response is quite adequate.

The difference in the observed flame structures are due to the presence of turbulence in the higher Reynolds number wake. Defining the length scale for a Kármán vortex street as $\ell \equiv U/f_s$, then for $U = 55$ cm/s and $f_s \approx 23$ s^{-1} then $\ell \approx 2.4$ cm, which corresponds to the cases of $Re_D = 73$ and 110. The laminar flame thickness is about 1 mm and since the only eddies present are of the scale $\ell = 2.4$ cm, then these flames would be expected to behave like wrinkled-laminar flames.

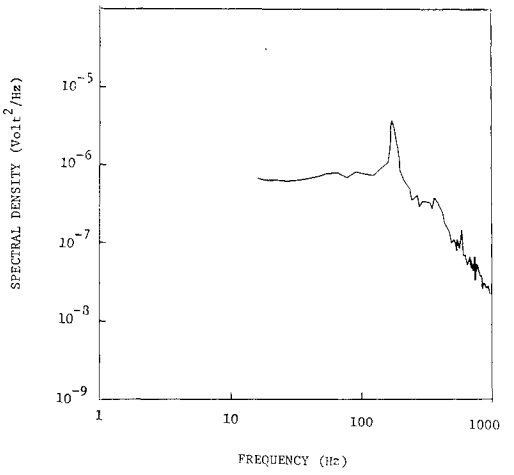

Fig. 9 Power spectrum of electrometer output for $Re_D = 500$ at $\tilde{c} = 0.19$.

This is consistent with the favorable comparison of the measured density statistics with the B-M-L model assuming small γ (see Fig. 6a).

For $U = 250$ cm/s and $f_s \approx 171$ s^{-1}, corresponding to $Re_D = 500$, $\ell \approx 1.5$ cm. This large value of ℓ might also indicate the existence of a wrinkled-laminar flame. However, as discussed in the introduction, at $Re_D = 500$ the wake contains significant turbulence and smaller scale eddies will be present. This distribution of scales is indicated in Fig. 9 by the energy at frequencies above 171 Hz where the peak occurs. For example, the power is reduced by two orders of magnitude at a frequency of 500 Hz for this case. In contrast, computed power spectra for the lower Reynolds number cases are reduced by three orders of magnitude at a frequency of 100 Hz. Therefore, the density fluctuations for the higher Re_D case results, in part, from turbulent eddies of scales much smaller than the coherent vortices at 171 Hz. These smaller eddies contribute a significant portion to the fluctuations in density. Taking 500 Hz as a representative frequency of these eddies, the associated eddy scale would be 5 mm which is of the order of magnitude of δ. This rough calculation indicates that the flame for this case is not a wrinkled-laminar flame since the flame is interacting with eddy motion whose scale is comparable to δ. This is consistent with the discrepancy between the measured statistics and the theory neglecting γ (see Fig. 6b).

Summary and Conclusions

Rayleigh scattering has been used to make nonintrusive space- and time-resolved density measurements in a flame interacting with a Kármán vortex street. The vortex shedding Reynolds numbers were 73, 110, and 500.

Spectral analysis of the Rayleigh scattering density measurements confirm that the dominant flame fluctuations occur at the vortex shedding frequency. The statistical properties of the density fluctuations were compared with the Bray-Moss-Libby model. Density statistics correlated well with $\tilde{c}$. For all cases the B-M-L model overpredicted density fluctuation intensities. The worst case was for the vortex shedding $Re_D = 500$ where the maximum was overpredicted by about 30%. The overprediction of density fluctuation intensities was not too severe for $Re_D = 73$ or 110. The differences in behavior between the flames for $Re_D = 73$ and 110 and the flame for $Re_D = 500$ were attributed to a breakdown of the wrinkled-laminar flame structure and the existence of distributed reaction zone for the latter case. On the other hand, the flames remained thin for the former cases and a flame sheet approximation remained valid. These conclusions are consistent with the existence and breakdown of a wrinkled-laminar flame structure.

Probability density functions of density were computed. From these the probabilities of products, reactants, and intermediates were determined. The probability of intermediates in the flame were found to be significant for all the cases studied. The maximum probability of intermediate states was about 40-50% for $Re_D = 73$ and 110, while for $Re_D = 500$ the maximum probability was found to be as high as 80%. It is clear that the flame sheet approximation used in the B-M-L model which neglects intermediate states, is not satisfactory in the latter case. However, the model was quite successful for the former cases. This is surprising since the values of γ in these flames are not very much smaller than 1.

Furthermore, this study has shown that the structure of approach flow will affect the flame behavior and γ. This limited study is not able to make a definitive statement on how γ behaves for different flows. In order for the B-M-L model to acocunt for effects of flow structure on flames, more experiments will be needed to ascertain the behavior of γ for flames in a variety of flows. More experimental data are required on the evolution of the pdf's for flames in different approach flows in order to construct appropriate models for flames in which significant intermediates are present.

Acknowledgments

This work was supported by the Air Force Office of Scientific Research under Contract F49620-80-C-0065. Additional support for equipment was provided by the Division of Basic Energy Sciences of the Department of Energy. Support for preparation of this manuscript was supplied by the Department of Mechanical Engineering and Mechanics, Drexel University. The experiments were performed at Lawrence Berkeley Laboratory, Berkeley, California.

References

[1] Karlovitz, B., "A Turbulent Flame Theory Derived from Experiments," *Selected Combustion Problems (AGARD)*, Butterworth, London, 1954, pp. 248-262.

[2] Scurlock, A. C. and Grover, J. H., "Experimental Studies on Turbulent Flames," *Selected Combustion Problems (AGARD)*, Buttersworth, London, 1954, pp. 215-247.

[3] Williams, F. A., *Combustion Theory*, Addison Wesley, Reading, Mass., 1965, Chap. 7.

[4] Andrews, G. E., Bradley, B., and Lwakabama, S. B., "Turbulence and Turbulent Flame Propagation—a Critical Appraisal," *Combustion and Flame*, Vol. 24, June 1975, pp. 285-304.

[5] Robben, F., "Comparison of Density and Temperature Measurement Using Raman Scattering and Rayleigh Scattering," Lawrence Berkeley Laboratory, Berkeley Calif., LBL-3294, Aug. 1975.

[6] Schefer, R. W., Robben, F., and Cheng, R. K., "Catalyzed Combustion of H_2/Air Mixtures in a Flat Plate Boundary Layer," *Combustion and Flame*, Vol. 38, No. 1, May 1980, pp. 51-63.

[7] Cheng, R. K., Bill, R. G. Jr., and Robben, F., "Experimental Study of Combustion in a Turbulent Boundary Layer," *18th Symposium (International) on Combustion*, The Combustion Institute, Pittsburgh, Pa., 1981, pp. 1021-1029.

[8] Karasalo, I. and Namer, I., "Numerical Study of a Flame in a Kámán Vortex Street," *Combustion and Flame*, Vol. 47, Sept. 1982, pp. 255-267.

[9] Ghoniem, A. F., Chorin, A. J., and Oppenheim, A. K., "Numerical Modeling of Turbulent Combusiton in Premixed Gases," *18th Symposium (International) on Combustion*, The Combustion Institute, Pittsburgh, Pa., 1981, pp. 1375-1383.

[10] Damkohler, G., "The Effect of Turbulence on the Flame Velocity in Gas Mixtures," English Transl., NACA TM 1112, April 1947.

[11] Williams, F. A., "Criteria for Existence of Wrinkled Laminar Flame Structure of Turbulent Premixed Flames," *Combustion and Flame*, Vol. 26, No. 2, April 1975, pp. 269-270.

[12] Chigier, N., *Energy Combustion and Environment*, McGraw-Hill, New York, 1981, Chap. 6.

[13] Karlovitz, B., Denniston, D. B., and Wells, F. E., "Investigation of Turbulent Flames, *Journal of Chemical Physics*, Vol. 19, No. 5, 1961, pp. 541-547.

[14] Scurlock, A. C. and Grover, J. H., "Propagation of Turbulent Flames," *4th Symposium (International) of Combustion*, Williams and Wilkins, Baltimore, Md., 1953, pp. 645-658.

[15] Bray, K. N. C. and Libby, P. A., "Interaction Effects in Premixed Turbulent Flames," *Physics of Fluids*, Vol. 19, No. 11, Nov. 1976, pp. 1687-1701.

[16] Gokalp, I., "On the Turbulence in Premixed Flames," *Acta Astronautica*, Vol. 6, July-Aug. 1979, pp. 847-860.

[17] Richmond, J. K., Singer, J. M., Cook, E. B., Oxendine, J. R., Grumer, J., and Burgess, D. S., "Turbulent Burning Velocities of Natural Gas-Air Flames with Pipe Flow Turbulence," *6th Symposium (International) on Combustion*, Reinhold, N. Y., 1956, pp. 303-311.

[18] Richmond, J. K., Grumer, J., and Burgess, D. S., "Turbulent Flame Propagation by Large-Scale Wrinkling of a Laminar Flame Front," *7th Symposium (International) on Combustion*, Buttersworth, London, 1958, pp. 615-620.

[19] Smith, K. O. and Gouldin, F. C., "Experimental Investigation of Flow Turbulence Effects on Premixed Methane-Air Flames," AIAA Paper 77-183, Jan. 1977.

[20] Bill, R. G. Jr., Namer, I., Talbot, L., Cheng, R. K., and Robben, F., "Flame Propagation in Grid-Induced Turbulence," *Combustion and Flame*, Vol. 43, No. 3, Dec. 1981, pp. 229-242.

[21] Marris, A. W., "A Review of Vortex Streets, Periodic Wakes, and Induced Vibrations," *Journal of Basic Engineering*, Vol. 86, 1964. pp. 185-196.

[22] Lamb, H., *Hydrodynamics*, Dover, New York, 1945, pp. 224-229.

[23] Friehe, C. A., "Vortex Shedding From Cylinders at Low Reynolds Numbers," *Journal of Fluid Mechanics*, Vol. 100, Pt. 2, 1980, pp. 237-241.

[24] Nishioka, M. and Sato, H., "Mechanism of Determination of the Shedding Frequency of Vortices Behind a Cylinder at Low Reynolds Numbers," *Journal of Fluid Mechanics*, Vol. 89, Pt. 1, 1978, pp. 49-63.

[25] Kovasznay, L. S. G., "Hot-Wire Investigation of the Wake Behind Cylinders at Low Reynolds Numbers," *Proceedings of the Royal Society (London) A*, Vol. 198, 1949, pp. 174-190.

[26] Roshko, A., "On the Development of Turbulent Wakes from Vortex Streets," NACA TN 2913, 1953.

[27] Roshko, A., "On the Drag and Shedding Frequency of Two-Dimensional Bluff Bodies," NACA TN 3169, 1954.

[28] Tritton, D. J., "Experiments on the Flow Past a Circular Cylinder at Low Reynolds Numbers," *Journal of Fluid Mechanics*, Vol. 6, 1959, pp. 547-567.

[29] Libby, P. A. and Bray, K. N. C., "Variable Density Effects in Premixed Turbulent Flames," *AIAA Journal*, Vol. 15, Aug. 1977, pp. 1186-1193.

[30] Bray, K. N. C. and Moss, J. B., "A Unified Statistical Model of the Premixed Turbulent Flame," *Acta Astonautica*, Vol. 4, March-April 1977, pp. 291-319.

[31] Pope, S. B., "The Statistical Theory of Turbulent Flames," *Philosphical Transactions of the Royal Society of London*, Vol. 291, No. 1384, July 1979, pp. 529-568.

[32] Namer, I., Agrawal, Y., Cheng, R. K., Robben, F., Schefer, R. W., and Talbot, L., "Interaction of a Flame Front With the Wake of a Cylinder," presented at the Fall meeting of the Western States Section/Combustion Institute, Stanford, Univ., Calif., Paper WSS/CI 77-50, Oct. 1977.

[33] Namer, I., "An Experimental Investigation of the Interaction Between a Kármán Vortex Sheet and a Premixed Laminar Flame," Ph.D. Thesis, Dept. of Mechanical Engineering, Univ. of Calif., Berkeley, Calif., 1980.

[34] Bill, R. G. Jr., Namer, I., Talbot, L., and Robben, F., "Density Fluctuations of Flames in Grid-Induced Turbulence," *Combustion and Flame*, Vol. 44, Jan. 1982, pp. 277-285.

[35] Namer, I., Bill, R. G. Jr., Talbot, L., and Robben, F., "Density Measurements in a Flame in a Kármán Vortex Street," presented at the Fall meeting of the Western States Section/Combustion Institute, Tempe, Ariz., Paper WSS/CI 81-37, Oct. 1981.

[36] Namer, I., Schefer, R. W., and Chan, M., "Interpretation of Rayleigh Scattering in a Flame," presented at the Spring meeting of the Western States Section/Combustion Institute, Stanford, Univ., Calif., Irvine, Calif., Paper WSS/CI 80-5, April 1980.